Determination of the thickness of air-water interface by Interfacial hydrogen bond dynamics

Gang Huang[1, a)] and Jie Huang[2, b)]
[1)] *Institute of Theoretical Physics, Chinese Academy of Sciences, Zhongguancun East Road 55, 100190 Beijing, China*
[2)] *Department of Physics, Wenzhou University, 325006 Wenzhou, China*

(Dated: 14 April 2022)

The thickness of the air-water interface can be determined by the interfacial hydrogen bond (IHB) dynamics. By density functional thoery-based molecular dynamics (DFTMD) simulations, two extreme cases of the interfacial HB dynamics are obtained: the former underestimates the HB breaking rate constant and the latter overestimates it. The interfacial HB dynamics in these two extreme cases tends to be the same as the thickness of the air-water interface increases to 4 Å. The interface thickness is determined when the interfacial HB dynamics under the two extreme cases are converged.

I. INTRODUCTION

It is widely accepted that water molecules behave differently at the interface than in bulk phase[1]. Estimating the thickness of the interface is a debated subject, and has been studied over the past years[2]. To estimate the interface thickness, Terahertz- spectroscopy methods and computer simulations have been employed. In computer simulations, the defined thickness of the interface depends on the parameters chosen manually, eg., the 10%–90% thickness[1,3,4]. However, the interface thickness, defined in terms of density, does not necessarily provide a reasonable distinction between bulk and interface dynamics. In addition, the density-based definition of interface thickness faces a debate over the reality of the oscillations of the density profile[5]. In this paper, combining *ab initio* molecular dynamics (AIMD) simulations and the calculation of instantaneous interface, we determine the thickness of air-water interface from the perspective of hydrogen bond (HB) dynamics. This method avoids the direct definition of interface thickness in terms of density, and naturally distinguishes the boundary between interfacial and bulk water.

Hydrogen bonds play a critical role in the behaviour of air-water interfaces[6–8]. There are many methods to study HB dynamics at the air-water interfaces, such as molecular dynamics simulation[6,9–12], neutron scattering[13–15], Infrared (IR) spectroscopy[16,17], and surface specific vibrational spectroscopy techniques[18–22]. Some experimental techniques, such as neutron reflection[23], have been used to measure the thickness of liquid-liquid interfaces. There are some general consensus on the fact that the thickness is about 3–10 Å[24,25]. There are already many works on the HB dynamics at the air-water interfaces[26,27]. However, these studies on the HB dynamics at the air-water interface did not give a method to extract interfacial H-bonds. In this work, we report a systematic approach to obtain the HB dynamics of the air-water interface and to determine the thickness of the interface, based on density functional-based molecular dynamics (DFMD) simulations (for details, see Appendix).

To determine interfacial H-bonds theoretically, we use two methods which are based on a newly defined Interfacial HB (IHB) population operator and Interfacial Molecule Sampling (IMS) at the interface, respectively. By IHB population method, the correlation functions of the *interface* HB population operator naturally derives the dynamic behavior of the H-bonds at the interface. Using the IMS method, we selected the water molecules (a set S_i) at the interface with thickness d at sampling time t_i, and calculated the statistical average value of the correlation functions of the HB population[28,29] over the sets $\{S_i\}$. These two methods give the HB dynamics of the air-water interface from two extreme cases. The combination of them has a "surface selectivity" to get more realistic HB dynamics of the interface, such as thickness of interfaces, HB lifetime and HB reaction rate constant.

The paper is organized as follows. In Sec. II we review the HB population operator and related correlation functions, and the method to obtain the HB breaking and reforming rate constants. Section III then introduces the ideas of IHB and IMS to define interfacial H-bonds. The main results and discussions are presented in Sec. IV. Finally, the conclusions are presented in Sec. V.

II. HYDROGEN BOND DYNAMICS

In this section, we will review general concepts in HB dynamics[28–30] used to analyze the structure and dynamics of bulk water and the air-water interface.

Using the geometric criterion of HB, Luzar and Chandler[28] have pioneered the analysis of HB dynamics of pure water, and subsequently such analysis was extended to more complex systems, e.g., electrolytes[31], protein[32] and micellar surfaces[33]. As stated in the criterion, two water molecules are H-bonded if their interoxygen distance between of specific tagged pair of water molecules is less than cutoff radius[34] $r_{OO}^c = 3.5$ Å and the O-H$\cdots$O angle is less than cutoff angle[35–38] $\phi^c = \pi/6$. We call this criterion of HB the Acceptor-Donor-Hydrogen (ADH) criterion. For comparison, we also use another definition of HB: when the distance between the O atoms of two water molecules is less than cutoff radius r_{OO}^c, and the O-H-O included angle is greater than cutoff angle $\theta^c = 2\pi/3$, then there is a HB between the two

[a)] Electronic mail: hg08@lzu.edu.cn
[b)] https://www.way2ml.com; Electronic mail: jichuang.wz@gmail.com

molecules. We denote this definition of HB as the Acceptor-Hydrogen-Donor (AHD) criterion.

We use a configuration $r(t)$ denotes the positions of all the atoms in the system at time t. Either of the criteria above allows us to define a HB population $h[r(t)] = h(t)$, which equals 1 when the particular tagged pair of molecules are bonded, and 0 otherwise. The fluctuation in $h(t)$ from its time-independent equilibrium average is defined by[30] $\delta h = h(t) - \langle h \rangle$. The probability that a specific pair of molecules is bonded in a large system is extremely small, then $\delta h(t) = h(t)$. Therefore, the correlation of $\delta h(t)$ can be written as

$$\langle \delta h(0) \delta h(t) \rangle = \langle h(0) h(t) \rangle,$$

where the averaging $\langle \cdots \rangle$ is to be performed over the ensemble of initial conditions.

A. Hydrogen bond correlation function $c(t)$, $k(t)$ and $n(t)$

The correlation function[31]

$$c(t) = \langle h(0) h(t) \rangle / \langle h \rangle$$

describes the structural relaxation of H-bonds. With the aid of the ergodic principle, the ensemble average $\langle \cdots \rangle$ is implemented by time average. The $\langle h \rangle$ is the probability that a pair of randomly chosen water molecules in the system is H-bonded at any time t. The $c(t)$ measures correlation in $h(t)$ independent of any possible bond breaking events, and it relaxes to zero, when t is large enough[39]. From $c(t)$, the HB relaxation time can be computed by $\tau_{\rm R} = \int t c(t) {\rm d}t / \int c(t) {\rm d}t$.

Because the thermal motion can cause distortions of H-bonds from the perfectly tetrahedral configuration, water molecules show a librational motion on a time scale of ~ 0.1 ps superimposed to rotational and diffusional motions (> 1 ps), which causes a time variation of interaction parameters. A new HB population $h^{(d)}(t)$ was also defined to obviate the distortion of real HB dynamics due to the above geometric definition[31,34]. The $h^{(d)}(t)$ is 1 when the interoxygen distance of a particular tagged pair of water molecules is less than $r_{\rm OO}^{\rm c}$ at time t, and 0 otherwise. The difference between the operators $h^{(d)}(t)$ and $h(t)$ is that those molecular pairs that meet the condition of $h^{(d)}(t) = 1$ may not meet the condition of $h(t) = 1$. In other words, the H-bonds between the tagged molecular pairs that satisfy the condition $h^{(d)}(t) = 1$ may have been broken, but they may more easily form H-bonds again. The function

$$c^{(d)}(t) = \langle h(0) h^{(d)}(t) \rangle / \langle h \rangle$$

is the probability that the specific two water molecules are located in reformable region ($r_{\rm OO} < r_{\rm OO}^{\rm c}$) at time t, if they were H-bonded at time zero. The correlation function

$$n(t) = \langle h(0)[1 - h(t)] h^{(d)}(t) \rangle / \langle h \rangle \qquad (1)$$

represents the probability at time t that a tagged pair of initially H-bonded water molecules are unbonded but remain separated by less than $r_{\rm OO}^{\rm c}$[31]. In the above formula, $1 - h(t)$ describes the breaking of a HB at time t after its formation at time $t = 0$.

To obtain the nature of H-bonds at the air-water interface, we calculated the reactive flux correlation function[40] and determine the rate constant ($1/\tau_{\rm HB}$), The rate of relaxation to equilibrium is characterized by the reactive flux,

$$k(t) = -\frac{{\rm d}c(t)}{{\rm d}t}, \qquad (2)$$

i.e., $\langle j(0)[1 - h(t)] \rangle / \langle h \rangle$, where $j(0) = -{\rm d}h/{\rm d}t|_{t=0}$ is the integrated flux departing the HB configuration space at time $t = 0$. The reactive flux $k(t)$ quantifies the rate that an initially present HB breaks at time t, independent of possible breaking and reforming events in the interval from 0 to t. Therefore, $k(t)$ measures the effective decay rate of an initial set of H-bonds[30,41].

For bulk water, there exists a ~ 0.2-ps transient period, during which the $k(t)$ quickly changes from its initial value[41]. However, at longer times, the $k(t)$ is independent of the HB definitions. Here, we performed a DFMD simulation of the bulk water system with a total time of 60 ps, and used two different HB definitions — ADH and AHD definition to calculate $k(t)$. We assume that each HB acts independently of other H-bonds[28,40], and due to detailed balance condition, we obtain $\tau_{\rm HB} = (1 - \langle h \rangle)/k$, where k is the rate constant of breaking a HB (forward rate constant)[42,43]. We use k' to represent the backward rate constant, i.e., the rate constant from the HB *on* state to the HB *off* state for a tagged pair of molecules.

B. Hydrogen bond breaking and reforming rate constants k and k'

Based on the functions $n(t)$, $h(t)$, $h^{(d)}(t)$, and $k(t)$, Khaliullin and Kühne[44] have obtain the ratio of HB breaking and reforming rate constants k/k' in bulk water, and then the lifetime and relaxation time of the HBs from simulation data. Here, for the air-water interface, we obtain the optimal solution range of k and k' from the relationship between the reactive flux $k(t)$ and the HB population correlation functions $c(t)$ and $n(t)$:

$$k(t) = k c(t) - k' n(t). \qquad (3)$$

We can find the optimal value of the rate constants, k and k', by a least squares fit of the calculated data $k(t)$, $c(t)$ and $n(t)$ beyond the transition phase. The function $c(t)$ can be regarded as a P-dimensional column vector composed by $(c_1, \cdots, c_P)^{\rm T}$, and denoted as $\mathbf{c}$, with c_i representing the value of the correlation $c(t)$ at $t = i$. Similarly, $n(t)$ and $k(t)$ can also be denoted as $\mathbf{n}$ and $\mathbf{k}$, respectively. Then, the rate constants k and k' can be determined from the matrix $\mathbf{A} = [\mathbf{c} \;\; \mathbf{n}]$:

$$\begin{bmatrix} k \\ -k' \end{bmatrix} = (\mathbf{A}^{\rm T}\mathbf{A})^{-1}\mathbf{A}^{\rm T}\mathbf{k}.$$

For bulk water and the air-water interface, the optimal k and k' are reported in Table I and II.

To obtain k and k', we performed the fitting in short and long time regions, respectively. We note that in the long time

TABLE I. The k and k' for the bulk water and the air-water interface (the time region 0.2 ps $< t <$ 2 ps).

Criterion	k (b)[a]	k' (b)	τ_{HB} (b)[b]	k (i)	k' (i)	τ_{HB} (i)
ADH	0.296	0.988	3.380	0.323	0.765	3.101
AHD	0.288	1.149	3.470	0.314	0.887	3.184

[a] The unit for k (k') is ps^{-1}. b: bulk; i: interface.
[b] The unit for τ_{HB} ($= 1/k$) is ps.

TABLE II. The k and k' for the bulk water and the air-water interface (the time region 2 ps $< t <$ 12 ps).

Criterion	k (b)	k' (b)	τ_{HB} (b)	k (i)	k' (i)	τ_{HB} (i)
ADH	0.115	0.039	8.718	0.157	0.068	6.372
AHD	0.105	0.047	9.496	0.155	0.088	6.472

region ($2 < t <$ 12 ps), the value of HB lifetime τ_{HB} is larger than that in short one ($0.2 < t <$ 2 ps), no matter for the bulk water or for the air-water interface. A larger τ_{HB} value means that the distance between a pair of water molecules stays within r_{OO}^c for a longer time.

III. HB DYNAMICS FOR INSTANTANEOUS AIR-WATER INTERFACE

A. Instantaneous air-water interface

Due to molecular motions, the identity of molecules that lie at the interface changes with time, and generally useful procedures for identifying interfaces must accommodate these motions. To determine the instantaneous air-water interface, we here adopt a spatial density-based method proposed by Willard and Chandler[45]. The coarse-grained density at space-time point $\mathbf{r},t$ can be expressed as polynmial

$$\bar{\rho}(\mathbf{r},t) = \sum_i \phi(|\mathbf{r} - \mathbf{r}_i(t)|;\xi),$$

where $\mathbf{r}_i(t)$ is the position of the i-th particle at time t and the sum is over all such particles, and

$$\phi(\mathbf{r};\xi) = (2\pi\xi^2)^{-3/2}\exp(-r^2/2\xi^2) \quad (4)$$

is a normalized Gaussian functions for a 3-dimensional system, where r is the magnitude of $\mathbf{r}$, and ξ is the coarse-graining length. Equation 4 is introduced to improve the accurancy of the interface, such that we can extend the domain and make it a single unicom, i.e., no cavity exists in the domain. With the parameter ξ set, the interfaces can be defined to be the 2-dimensional manifold $\mathbf{r} = \mathbf{s}$ such that

$$\bar{\rho}(\mathbf{s};t) = \rho_c \quad (5)$$

where ρ_c is a reference density. This interface is a function of time as molecular configurations changes with time, that is $\mathbf{s}(t) = \mathbf{s}(\{\mathbf{r}_i(t)\})$.

For a given molecular configuration $\{\mathbf{r}_i(t)\}$, Eq. 5 can be solved through interpolation on a spatial grid[45]. Figure 1 illustrates the obtained interfaces for one configuration of a slab of pure water. We have taken $\{\mathbf{r}_i(t)\}$ to refer to the positions of all O atoms in the system, and because the bulk correlation length of liquid water is about one molecular diameter, we have used ξ =2.4 Å; further, we have used $\rho_c = 0.016$ Å^{-3}, which is approximately one-half the bulk density of water[45].

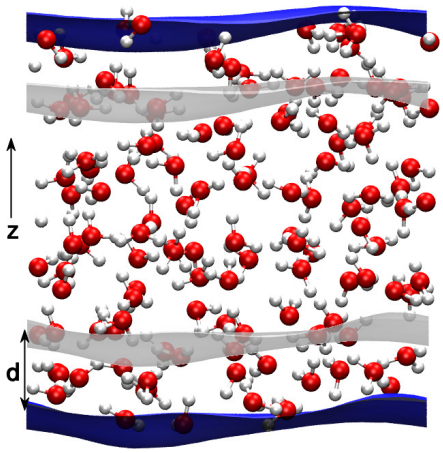

FIG. 1. A slab of water with the instantaneous surface $\mathbf{s}$ represented as a blue mesh on the upper and lower phase boundary. The normal is along the z-axis and d is the thickness of the interface. The grey surface is obtained by translating the surface to the inside of the system along the z-axis by d.

For the slab in the cuboid simulation box, we can get another surface $\mathbf{s}_0(t)$ by translating the surface $\mathbf{s}(t)$ along the system's normal (into bulk) to a distance d. The region between the two surfaces $\mathbf{s}(t)$ and $\mathbf{s}_0(t)$ is defined as *the air-water interface*.

B. Hydrogen bond dynamics at the instantaneous air-water interface: two extreme cases

1. Hydrogen bond dynamics from Interfacial HB population

After determining the interface, we can define the interfacial HB population operator $h^{(s)}[\mathbf{r}(t)]$ as follows: It has a value 1 when the particular tagged molecular pair i,j are H-bonded *and* both molecules are inside the interface with a thickness d, and 0 otherwise:

$$h^{(s)}[\mathbf{r}(t)] = \begin{cases} 1 & i,j \text{ are H-bonded, } \textit{and} \\ & i,j \text{ are at the interface;} \\ 0 & \text{otherwise.} \end{cases} \quad (6)$$

Using $h^{(s)}(t)$, we define the correlation function $c^{(s)}(t)$ that describes the fluctuation of H-bonds *at the interface*:

$$c^{(s)}(t) = \langle h^{(s)}(0)h^{(s)}(t)\rangle / \langle h^{(s)}\rangle. \quad (7)$$

Similar to Eq. 1 and Eq. 2, we further define correlation functions

$$n^{(s)}(t) = \langle h^{(s)}(0)[1 - h^{(s)}(t)]h^{(d,s)}\rangle / \langle h^{(s)}\rangle, \quad (8)$$

and

$$k^{(s)}(t) = -\frac{dc^{(s)}(t)}{dt}. \quad (9)$$

The $h^{(d,s)}(t)$ is 1 when the a particular tagged pair of water molecules i, j are *at the interface* and the interoxygen distance between the two molecules is less than r_{OO}^{c} at time t, and 0 otherwise, i.e.,

$$h^{(d,s)}[\mathbf{r}(t)] = \begin{cases} 1 & i,j \text{ are at the interface} \\ & \text{and } |O_iO_j| < r_{OO}^{c}; \\ 0 & \text{otherwise.} \end{cases}$$

Therefore, $n^{(s)}(t)$ represents the prabability at time t that a tagged pair of initially H-bonded water molecules at the interface are unbonded but remain at the interface and separated by less than r_{OO}^{c}; $k^{(s)}(t)$ measures the effective decay rate of H-bonds at the interface. The functions defined in Eq.7–9 can be used to determine the reaction rate constant of breaking and reforming and the lifetimes of H-bonds at the interface.

2. *Hydrogen bond dynamics from molecule sampling*

As the second method to extract H-bonds at the interface, we further sampling the molecules at the instantaneous interface, using the following procedure :

1. Define an interface with a thickness d (see Fig. 1).
2. For each observation time $t_i (i = 1, \cdots, N)$, select a set S_i of water molecules which are at the interface, and calculate the HB dynamics for the molecules that belong to S_i.
3. S_i can be determined for each time t_i. Therefore, we calculated the correlation functions $c(t)$, $n(t)$ and $k(t)$ for the molecules belong to S_i for the simulated trajectory with length t_e.
4. Averaged the correlation functions obtained over S_i.

IV. DISCUSSIONS: EFFECTS OF AIR-WATER INTERFACE ON HYDROGEN BOND DYNAMICS

A. Hydrogen bond relaxation

Two geometric criteria of H-bonds are used to calculate the $h^{(s)}(t)$, and the corresponding $c^{(s)}(t)$ from Eq.7 are shown in Fig. 2. We found that as d increases, $c^{(s)}(t)$ at the interface relaxes more slowly. When d is greater than 4 Å, $c^{(s)}(t)$ approaches a stable function, i.e., it recovers the bulk value. The behavior is independent of the HB definition as shown by the comparison of results in panel a and b of Fig. 2. Similarly, Fig.3 shows the d-dependence of $c(t)$. Comparing Fig.s 2 and 3, We also find that $c(t)$ has similar characteristics to $c^{(s)}(t)$: as d increases, $c(t)$ also relaxes more slowly; When d is greater than 4 Å, $c^{(s)}(t)$ also approaches a stable function.

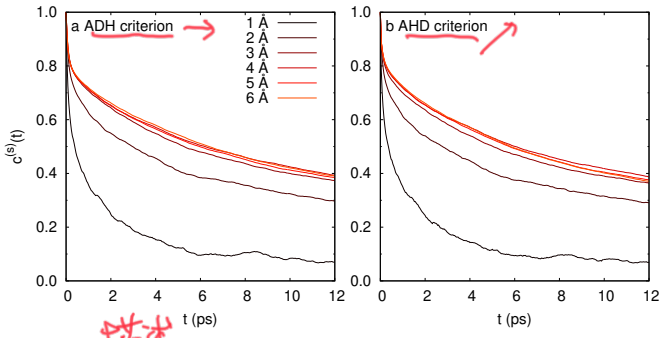

FIG. 2. The $c^{(s)}(t)$ for interfacial H-bonds with differnt thickness (d), based on HB population operator $h^{s}(t)$, as computed from the (a) ADH and (b) AHD criteria of H-bonds.

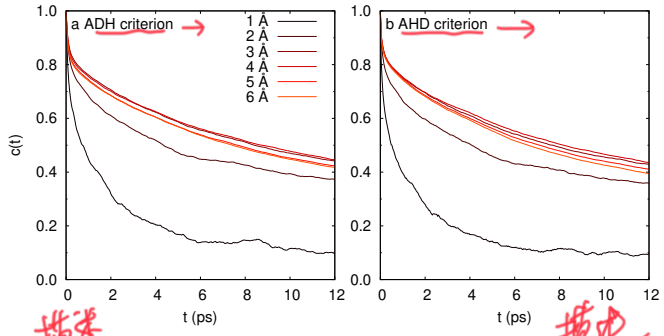

FIG. 3. The $c(t)$ for H-bonds at the interfaces with different d, based on HB population operator $h(t)$, as computed from the (a) ADH and (b) AHD criteria of H-bonds. These results are based on the IMS method, in which the sampling is performed every 4 ps.

Comparing $c(t)$ and $c^{(s)}(t)$, the second feature is that for the same d, the value of $c(t)$ is always slightly larger than $c^{(s)}(t)$. Moreover, regardless of the AHD or ADH criteria of a HB, these two features are valid. The first feature is the general one of interfacial H-bonds, while the second feature is derived from the difference in the definitions of HB population operators $h(t)$ and $h^{(s)}(t)$. Using this difference between $h(t)$ and $h^{(s)}(t)$, we can obtain the hydrogen bonding dynamics of the real interface, especially the thickness of the interface.

B. Hydrogen bond breaking and reforming rate constants k and k'

To find the reaction rate constants k and k', we can start from the correlation functions $c^{(s)}(t)$, $n^{(s)}(t)$ and $k^{(s)}(t)$, (or $c(t)$, $n(t)$ and $k(t)$) of the H-bonds that are at the interface at time t. Figure 4 compares the rate constants (k and k') and the lifetime τ_{HB} obtained by the IHB and interfacial molecule selection (IMS) methods. We found that, for all the three quantities k, k' and τ_{HB}, the behavior as function of the thickness of the interface is only slightly affected by the calculation methods. To illustrate this point more clearly, we compare the k, k' and τ_{HB} obtained under the two methods.

As we can see from Fig. 4, when d is larger than d_0 =4

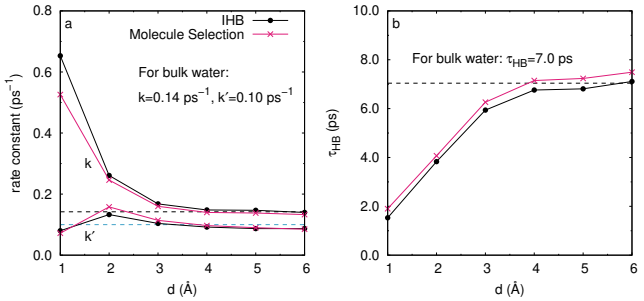

FIG. 4. The dependence of (a) the rate constants k and k' and (b) the HB lifetime τ_{HB} on the interface thickness, obtained by the IHB and the IMS method, respectively. The corresponding k, k' and τ_{HB} in bulk water are also drawn with dashed lines as a reference. In sub-figure (a), the k of bulk water is represented by a black dashed line, and the k' by a blue dashed line; in sub-figure (b), the τ_{HB} of bulk water is represented by a black dashed line. The ADH criterion is used and the fits are carried on the time region 0.2 ps $< t <$ 12 ps.

Å, the constants k and k' obtained by the two methods agree quantitatively.

When we look at the molecules at the interface with thickness less than d_0, the values of the rate constants depend on the method. The k obtained by using the IHB method is relatively larger than that from the IMS method, and k' is relatively smaller. Since $\tau_{\mathrm{HB}} = 1/k$, this directly leads to a relatively shorter HB lifetime using the IHB method. This result is related to the definitions of $h(t)$ and $h^{(\mathrm{s})}(t)$. The definition of $h^{(\mathrm{s})}(t)$ makes the HB break rate at the interface artificially increased. At the same time, the IMS method, which is based on $h(t)$, retains the original rate constant of H-bonds, but it may include the contribution of bulk water molecules to the rate constant.

In Fig. 4, the k, k' and τ_{HB} for the *bulk* water are also drawn with dashed lines as a reference. Comparing the above-mentioned physical quantities at the air-water interface and bulk water, we found that when the interface thickness is larger than 4 Å, no matter which statistical method is used, the obtained reaction rate constants of the interface water is *greater* than that in bulk water. Therefore, the HB lifetime $\tau_{\mathrm{HB}} = 1/k$ in interface water is smaller than that in bulk water.

Furthermore, we find from Fig. 4 that as d increases, k and k' also tend to the rates in bulk water at the same condition. These results are obtained by the least squares method in the same interval (0.2–12 ps). They show that the IHB method can get as good results as the IMS method when d is larger than 4 Å.

The above two methods respectively give an extreme case of interface HB dynamics. In the IMS method, since the configuration of molecules changes over time, the contribution of H-bonds in bulk phase is included. In the IHB method, it is accurate to choose the water molecules and H-bonds at the interface, but some H-bonds at the interface is artificially destroyed. In other words, the calculated HB dynamics obtained by IHB method is *accelerated*, compared to the real one. Real HB dynamics of the interface is between the results of the above two methods. Therefore, we can approximate the true HB dynamics of the interface, by combining both the IHB and IMS methods. In these two extreme cases the interfacial HB characteriestics tends to be the same as the thickness of the interface increases. Properties such as the HB lifetime, HB reaction rate constants, and the thickness of the air-water interface can be estimated. For example, as the parameter d increases, when all the k, k', τ_{HB} of the interface calculated by both methods become consistent, the value of d can be considered equal to the true thickness of the air-water interface.

V. CONCLUSIONS

Based on the DFTMD simulations, the IMS method can partially gives information on the HB breaking and reforming reaction rate constants through the air-water interface and therefore partially shows how much the interface affects the dynamics of H-bonds in water. It *understimates* the HB breaking rate constant of the interface.

The IHB method also provide the interfacial HB dynamics of the air-water interfaces. It also provides partial information on the HB breaking and reforming reaction rates at the interface. However, it *overestimates* the HB breaking rate constant.

As the thickness of the interface increases, comparing the calculation results in the two extreme cases, we found that the HB breaking and reforming rate constants in the *water layer below the surface* tends to be uniform (see Fig.4a). Therefore, the real HB dynamical characteristics at the air-water interface can be derived. We conclude that from the perspective of HB dynamics, the thickness of the air-water interface is about 4 Å. In other words, at thickness ~ 4 Å the properties of the air-water interface layer become the same as for bulk water. This value has reference significance for the study of the influence of ions on the H-bonds outside solvation shells of ions.

The idea of combination of IHB and IMS can naturally be extended to the solution interface. This method of determining interfacial thickness using interfacial HB dynamics can be extended to other interfacial systems, so that the boundary between the interface and the bulk phase can be naturally determined. For the systems where the statistical properties of the interface and bulk phase differ significantly[46,47], these differences will be represented more appropriately. In addition, the IHB method itself can also be extended. One can combine Luzar-Chandler HB population with different environment, eg., the hydration shell of ions.

ACKNOWLEDGMENTS

The simulations were performed on the Mogon ZDV cluster in Mainz and on the Cray XE6 (Hermit) at the HRLS supercomputing center in Stuttgart.

Appendix: Computational details

To describe the subtleties of H-bonding in water[48], we have performed a DFMD simulation[49] for bulk water and

the air-water interface. This simulation makes use of some technologies that have been successfully tested on water and solutions[50–53], namely the Goedecker-Teter-Hutter (GTH) pseudopotentials[54–56], Generalised Gradient Approximation (GGA) of the exchange-correlation functional[57,58], and dispersion force correction, DFT-D3[59,60]. By eliminating the strongly bound core electrons, the GTH pseudopotentials reduce the number of occupied electronic orbitals that have to be treated in an electronic structure calculation. There are dual-space Gaussian-type pseudopotentials that are separable and satisfy a quadratic scaling with respect to system size[61]. The GGA functionals generally describe the dipole and quadruple moments of the molecules quite well; and DFT-D3 correction can treat the van der Waals dispersion forces in Density Functional Theory (DFT) and improve the structural properties without more computational cost, and thus can be used at the air-water interface.

The DFMD calculation is implemented by a NVT code that implemented in the CP2K/QUICKSTEP package[62,63]. The BLYP XC functional, which consists of Becke non-local exchange[57] and Lee-Yang-Parr correlation[58] have been employed. The electron-ion interactions are described by GTH pseudopotentials[55,64]. A Gaussian basis for the wave functions and an auxiliary plane wave bisis set for the density are used in this scheme. DZVP-GTH basis set is used for all atoms and a cutoff of 280 Ry is chosen for the charge density[62]. The Nosé-Hoover chain thermostat[65] is used to conserve the temperature at 300 K. The simulation for the air-water interface use a time step of 0.5 fs.

The bulk water system consisted of 128 water molecules in a periodic box of size $15.64 \times 15.64 \times 15.64$ Å^3, and with a density of 1.00 g cm^{-3}. The slab consisted of 128 water molecules in a periodic box of size $15.64 \times 15.64 \times 31.28$ Å^3. The length of each trajectory in each simulation is 60 ps.

The RDFs $g_{\mathrm{OO}}(r)$ and $g_{\mathrm{OH}}(r)$ for the bulk water systems are shown in Fig. 5. The probability distribution of O and H atoms in the simulated model of air-water interface is showed in Fig. 6.

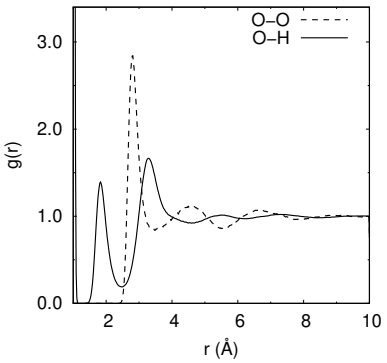

FIG. 5. The partial RDFs for the simulated bulk water system.

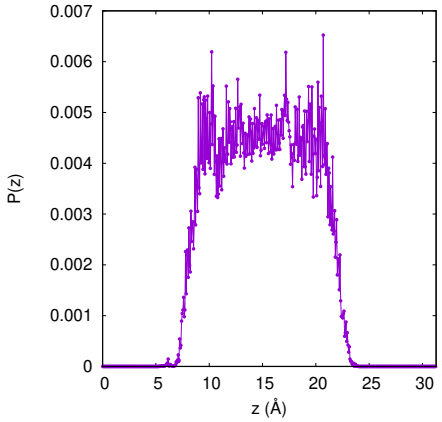

FIG. 6. Probability distribution $P(z)$, along the z-axis, of H_2O in the slab.

[1] L. X. Dang and T.-M. Chang, "Molecular dynamics study of water clusters, liquid, and liquid-vapour interface of water with many-body potentials," J. Chem. Phys. **106**, 8149 (1997).

[2] P. K. Nandi, N. J. English, Z. Futera, and A. Benedetto, "Hydrogen-Bond Dynamics at the Bio-Water Interface in Hydrated Proteins: A Molecular-Dynamics Study," Phys. Chem. Chem. Phys. **19**, 318–329 (2017).

[3] D. Beaglehole and P. Wilson, "Thickness and Anisotropy of the Ice-Water Interface," J. Phys. Chem. **97**, 11053–11055 (1993).

[4] T. D. Kühne, T. A. Pascal, E. Kaxiras, and Y. Jung, "New Insights into the Structure of the Vapor/Water Interface from Large-Scale First-Principles Simulations," J. Phys. Chem. Lett. **2**, 105–113 (2011).

[5] R. Evans, J. Henderson, D. Hoyle, A. Parry, and Z. Sabeur, "Asymptotic decay of liquid structure: oscillatory liquid-vapour density profiles and the Fisher-Widom line," Molecular Phys. **80**, 755–775 (1993).

[6] J. Chowdhary and B. M. Ladanyi, "Hydrogen bond dynamics at the water/hydrocarbon interface," J. Phys. Chem. B **113**, 4045–4053 (2008).

[7] K. ichi Inoue, M. Ahmed, S. Nihonyanagi, and T. Tahara, "Reorientation-induced relaxation of free OH at the air/water interface revealed by ultrafast heterodyne-detected nonlinear spectroscopy," Nature Communications **11**, 5344 (2020).

[8] D. Ojha and T. Kühne, "Hydrogen bond dynamics of interfacial water molecules revealed from two-dimensional vibrational sum-frequency generation spectroscopy," Sci. Rep. **11**, 2456 (2021).

[9] A. Tongraar, P. Tangkawanwanit, and B. M. Rode, "A Combined QM/MM Molecular Dynamics Simulations Study of Nitrate Anion (NO_3^-) in Aqueous Solution," J. Phys. Chem. A **110**, 12918–12926 (2006).

[10] J. Chanda and S. Bandyopadhyay, "Hydrogen Bond Lifetime Dynamics at the Interface of a Surfactant Monolayer," J. Phys. Chem. B **110**, 23443–23449 (2006).

[11] A. Tongraar, S. Hannongbua, and B. M. Rode, "QM/MM MD Simulations of Iodide Ion (I-) in Aqueous Solution: A Delicate Balance Between Ion-Water and Water-Water H-bond Interactions," J. Phys. Chem. A **114**, 4334–4339 (2010).

[12] P. Banerjee, S. Yashonath, and B. Bagchi, "Coupled jump rotational dynamics in aqueous nitrate solutions," J. Chem. Phys. **145**, 234502 (2016), https://aip.scitation.org/doi/pdf/10.1063/1.4971864.

[13] S.-H. Chen, K. Toukan, C.-K. Loong, D. L. Price, and J. Teixeira, "Hydrogen-bond spectroscopy of water by neutron scattering," Phys. Rev. Lett. **53**, 1360–1363 (1984).

[14] J. Teixeira and M. C. Bellissent-Funel, "Dynamics of water studied by neutron scattering," Journal of Physics: Condensed Matter **2**, SA105–SA108 (1990).

[15] M.-C. Bellissent-Funel and J. Teixeira, "Dynamics of water studied by coherent and incoherent inelastic neutron scattering," Journal of Molecular Structure **250**, 213–230 (1991).

[16] J. C. Werhahn, S. Pandelov, S. S. Xantheas, and H. Iglev, "Dynamics of weak, bifurcated, and strong hydrogen bonds in lithium nitrate trihydrate," J. Phys. Chem. Lett. **2**, 1633–1638 (2011).

[17] J. A. Fournier, W. Carpenter, L. D. Marco, and A. Tokmakoff, "Interplay of ion-water and water-water interactions within the hydration shells of nitrate and carbonate directly probed with 2d ir spectroscopy," J. Am. Chem. Soc. **138**, 9634–9645 (2016).

[18] A. M. Jubb, W. Hua, and H. Allen, "Environmental chemistry at vapor/water interfaces: Insights from vibrational sum frequency generation spectroscopy," Ann. Rev. Phys. Chem. **63**, 107–130 (2012).

[19] H.-F. Wang, L. Velarde, W. Gan, and L. Fu, "Quantitative sum-frequency generation vibrational spectroscopy of molecular surfaces and interfaces: Lineshape, polarization, and orientation," Annual Review of Physical Chemistry **66**, 189–216 (2015).

[20] Y.-C. Wen, S. Zha, X. Liu, S. Yang, P. Guo, G. Shi, H. Fang, Y. R. Shen, and C. Tian, "Unveiling microscopic structures of charged water interfaces by surface-specific vibrational spectroscopy," Phys. Rev. Lett. **116**, 016101 (2016).

[21] T. Ishiyama and A. Morita, "Computational analysis of vibrational sum frequency generation spectroscopy," Annual Review of Physical Chemistry **68**, 355–377 (2017).

[22] C. Peñalber-Johnstone, G. Adamová, N. V. Plechkova, M. Bahrami, T. GhaedSharaf, M. H. Ghatee, K. R. Seddon, and S. Baldelli, "Sum frequency generation spectroscopy of tetraalkylphosphonium ionic liquids at the air-liquid interface," J. Chem. Phys. **148**, 193841 (2018), https://doi.org/10.1063/1.5009674.

[23] L. T. Lee, D. Langevin, and B. Farnoux, "Neutron reflectivity of an oil-water interface," Phys. Rev. Lett. **67**, 2678–2681 (1991).

[24] S. Pezzotti, D. R. Galimberti, and M.-P. Gaigeot, "2D H-Bond Network as the Topmost Skin to the Air-Water Interface," J. Phys. Chem. Lett. **8**, 3133–3141 (2017).

[25] Y. Peng, Z. Tong, Y. Yang, and C. Q. Sun, "The Common and Intrinsic Skin Electric-Double-Layer (EDL) and Its Bonding Characteristics of Nanostructures," Applied Surface Science **539**, 148208 (2021).

[26] P. Liu, E. Harder, and B. J. Berne, "Hydrogen-Bond Dynamics in the Air-Water Interface," J. Phys. Chem. B **109**, 2949–2955 (2005).

[27] S. J. Irudayam and R. H. Henchman, "Long-range hydrogen-bond structure in aqueous solutions and the vapor-water interface," J. Chem. Phys. **137**, 034508 (2012).

[28] A. Luzar and D. Chandler, "Effect of environment on hydrogen bond dynamics in liquid water," Phys. Rev. Lett. **76**, 928–931 (1996).

[29] A. Luzar, "Water Hydrogen-Bond Dynamics Close to Hydrophobic and Hydrophilic groups," Faraday Discuss. **103**, 29–40 (1996).

[30] D. Chandler, *Introduction to Morden Statistical Mechanics* (Oxford University press, Oxford, 1987).

[31] A. Chandra, "Effects of Ion Atmosphere on Hydrogen-Bond Dynamics in Aqueous Electrolyte Solutions," Phys. Rev. Lett. **85**, 768–771 (2000).

[32] M. Tarek and D. J. Tobias, "Role of Protein-Water Hydrogen Bond Dynamics in the Protein Dynamical Transition," Phys. Rev. Lett. **88**, 138101 (2002).

[33] S. Pal, B. Bagchi, and S. Balasubramanian, "Hydration Layer of a Cationic Micelle, C_{10}TAB: Structure, Rigidity, Slow Reorientation, Hydrogen Bond Lifetime, and Solvation Dynamics," J. Phys. Chem. B **109**, 12879–12890 (2005).

[34] F. Sciortino and S. L. Fornili, "Hydrogen Bond Cooperativity in Simulated Water: Time Dependence Analysis of Pair Interactions," J. Chem. Phys. **90**, 2786–2792 (1989).

[35] A. K. Soper and M. G. Phillips, "A New Determination of the Structure of Water at 25 ° C," Chem. Phys **107**, 47–60 (1986).

[36] J. Teixeira, M. C. Bellisent-Funel, and S. H. Chen, "Dynamics of Water Studied by Neutron Scattering," J. Phys. Condens. Matter **2**, SA105 (1990).

[37] A. Luzar and D. Chandler, "Structure and hydrogen bond dynamics of water-dimethyl sulfoxide mixtures by computer simulations," J. Chem. Phys. **98**, 8160–8173 (1993).

[38] S. Balasubramanian, S. Pal, and B. Bagchi, "Hydrogen-Bond Dynamics Near a Micellar Surface: Origin of the Universal Slow Relaxation at Complex Aqueous Interfaces," Phys. Rev. Lett. **89**, 115505 (2002).

[39] D. C. Rapaport, "Hydrogen Bonds in Water: Network Organization and Lifetimes," Mol. Phys. **50**, 1151–1162 (1983).

[40] A. Luzar, "Resolving the Hydrogen Bond Dynamics Conundrum," J. Chem. Phys. **113**, 10663 (2000).

[41] F. W. Starr, J. K. Nielsen, and H. E. Sta, "Hydrogen-Bond Dynamics for the Extended Simple Point-Charge Model of Water," Phys. Rev. E **62**, 579–587 (2000).

[42] D. Chandler, "Roles of Classical Dynamics and Quantum Dynamics on Activated Processes Occurring in Liquids," J. Stat. Phys. **42**, 49–67 (1986).

[43] D. Chandler, "Statistical Mechanics of Isomerization Dynamics in Liquids and the Transition State Approximation," J. Chem. Phys. **68**, 2959–2970 (1978).

[44] R. Z. Khaliullin and T. D. Kühne, "Microscopic properties of liquid water from combined ab initio molecular dynamics and energy decomposition studies," Phys. Chem. Chem. Phys. **15**, 15746–15766 (2013).

[45] A. P. Willard and D. Chandler, "Instantaneous Liquid Interfaces," J. Phys. Chem. B **114**, 1954 (2010).

[46] L. Zhu, C. W. Brian, S. F. Swallen, P. T. Straus, M. D. Ediger, and L. Yu, "Surface self-diffusion of an organic glass," Phys. Rev. Lett. **106**, 256103 (2011).

[47] W. Zhang and L. Yu, "Surface diffusion of polymer glasses," Macromolecules **49**, 731 (2016).

[48] K. Laasonen, M. Sprik, M. Parrinello, and R. Car, ""ab initio" liquid water," J. Chem. Phys. **99**, 9080–9089 (1993), https://doi.org/10.1063/1.465574.

[49] D. Marx and J. Hutter, "Ab Initio Molecular Dynamics: Theory and Implemention," Modern Methods and Algorithms of Quantum Chemistry, J.Grotendorst (Ed.) John von Neumann Institute for Computing, Jülich, NIC Series **1**, 301–499 (2000).

[50] R. Khatib, E. H. G. Backus, M. Bonn, M. Perez-Haro, M.-P. Gaigeot, and M. Sulpizi, "Water Orientation and Hydrogen-Bond Structure at the Fluorite/Water Interface," Scientific Reports **6**, 24287 (2016).

[51] R. Khatib, T. Hasegawa, M. Sulpizi, E. H. G. Backus, M. Bonn, and Y. Nagata, "Molecular Dynamics Simulations of SFG Librational Modes Spectra of Water at the Water-Air Interface," J. Phys. Chem. C **120**, 18665–18673 (2016).

[52] R. Khatib and M. Sulpizi, "Sum Frequency Generation Spectra from Velocity-Velocity Correlation Functions," J. Phys. Chem. Lett. **8**, 1310–1314 (2017).

[53] M. Sulpizi, M. Salanne, M. Sprik, and M.-P. Gaigeot, "Vibrational sum frequency generation spectroscopy of the water liquid-vapor interface from density functional theory-based molecular dynamics simulations," J. Phys. Chem. Lett. **4**, 83–87 (2013), http://dx.doi.org/10.1021/jz301858g.

[54] S. Goedecker, M. Teter, and J. Hutter, "Separable dual-space gaussian pseudopotentials," Phys. Rev. B **54**, 1703–1710 (1996).

[55] C. Hartwigsen, S. Goedecker, and J. Hutter, "Relativistic separable dual-space gaussian pseudopotentials from H to Rn," Phys. Rev. B **58**, 3641–3662 (1998).

[56] M. Krack, "Pseudopotentials for H to Kr optimized for gradient-corrected exchange-correlation functionals," Theor. Chem. Acc. **114**, 145–152 (2005).

[57] A. D. Becke, "Density-functional exchange-energy approximation with correct asymptotic behavior," Phys. Rev. A **38**, 3098 (1988).

[58] C. Lee, W. Yang, and R. G. Parr, "Development of the colic-salvetti correlation-energy formula into a functional of the electron density," Phys. Rev. B **37**, 785 (1988).

[59] S. Grimme, J. Antony, S. Ehrlich, and H. Krieg, "A Consistent and Accurate Ab Initio Parametrization of Density Functional Dispersion Correction (DFT-D) for the 94 Elements H-Pu," J. Chem. Phys. **132**, 154104 (2010).

[60] J. Klimeš and A. Michaelides, "Perspective: Advances and Challenges in Treating van der Waals Dispersion Forces in Density Functional Theory," J. Chem. Phys. **137**, 120901–120912 (2012).

[61] J.-B. Lu, D. C. Cantu, M.-T. Nguyen, J. Li, V.-A. Glezakou, and R. Rousseau, "Norm-Conserving Pseudopotentials and Basis Sets To Explore Lanthanide Chemistry in Complex Environments," J. Chem. Theory Comput. **15**, 5987–5997 (2019).

[62] J. VandeVondele, M. Krack, F. Mohamed, M. Parrinello, T. Chassaing, and J. Hutter, "Quickstep: Fast and accurate density functional calculations using a mixed gaussian and plane waves approach," Comput. Phys. Commun. **167**, 103–128 (2005).

[63] T. D. Kühne, M. Iannuzzi, M. Del Ben, V. V. Rybkin, P. Seewald, F. Stein, T. Laino, R. Z. Khaliullin, O. Schütt, F. Schiffmann, D. Golze, J. Wilhelm, S. Chulkov, M. H. Bani-Hashemian, V. Weber, U. Borštnik, M. Taillefumier, A. S. Jakobovits, A. Lazzaro, H. Pabst, T. Müller, R. Schade, M. Guidon, S. Andermatt, N. Holmberg, G. K. Schenter, A. Hehn, A. Bussy, F. Belleflamme, G. Tabacchi, A. Glöß, M. Lass, I. Bethune, C. J. Mundy, C. Plessl, M. Watkins, J. VandeVondele, M. Krack, and J. Hutter, "Cp2k: An electronic structure and molecular dynamics software package - quickstep: Efficient and accurate electronic structure calculations," J. Chem. Phys. **152**, 194103 (2020), https://doi.org/10.1063/5.0007045.

[64] G. Lippert, J. Hutter, and M. Parrinello, "The gaussian and augmented-

plane-wave density functional method for ab initio molecular dynamics simulations," Theor. Chem. Acc. **103**, 124 (1999).

[65] G. J. Martyna, M. L. Klein, and M. Tuckerman, "Nosé-hoover chains: The canonical ensemble via continuous dynamics," J. Chem. Phys. **97**, 2635 (1992).